Excessive repolarization-dependent calcium currents induced by strong depolarizations in rat skeletal myoballs

Andrea Fleig and Reinhold Penner

Department of Membrane Biophysics, Max-Planck-Institute for Biophysical Chemistry, Am Fassberg, 37077 Göttingen, Germany

1. Whole-cell patch-clamp recordings were used to study voltage-dependent Ca^{2+} currents in skeletal myoballs cultured from newborn rats.

2. Depolarizing voltage pulses evoked classical L-type Ca^{2+} currents, whereas repolarization induced tail currents, whose properties deviated from the expected behaviour of the preceding Ca^{2+} currents in both voltage dependence and kinetics.

3. Depolarizations of up to +10 mV primarily recruited tail currents that correspond to the Ca^{2+} channels activated and conducting during the depolarizing pulse, but stronger depolarizations yielded an additional tail current component that exceeded the 'normal' tail current amplitude by several-fold.

4. Activation kinetics of the tail currents were biexponential, with a fast time constant matching the activation time course of the pulse currents ($\tau \approx 40$ ms) and an additional slower component with a voltage-dependent time course that had no kinetic counterpart in the pulse currents ($\tau \approx 150$–600 ms).

5. Both pulse and tail currents were blocked by the dihydropyridine, PN200-110, suggesting that they represent Ca^{2+} channels of the L-type.

6. We suggest the presence of at least two subsets of dihydropyridine-sensitive Ca^{2+} channels in skeletal muscle cells. One subset has classical L-type channel characteristics and the other has anomalous gating behaviour that is 'activated' or 'primed' by strong and long-lasting depolarizations without conducting significant Ca^{2+} current – however, upon repolarization, this subset of channels generates large tail currents.

The functional role of dihydropyridine receptors (DHPRs) in skeletal muscle is not entirely understood (Rios & Pizarro, 1991; Lamb, 1992). It is thought that DHPRs can function as both voltage-activated calcium channels and voltage sensors mediating depolarization-induced calcium release from the sarcoplasmic reticulum (Schneider & Chandler, 1973; Melzer, Schneider, Simon & Szucs, 1986; Rios & Brum, 1987). Concerning skeletal muscle cells, there is some debate as to whether there is a discrepancy between dihydropyridine binding sites and conducting ion channels (reviewed by Lamb & Walsh, 1987). The sarcolemma of mammalian skeletal muscle expresses voltage-dependent, 'slow' L-type Ca^{2+} channels with activation time constants around 50 ms (Donaldson & Beam, 1983; Beam, Knudson & Powell, 1986; Cognard, Lazdunski & Romey, 1986). Calcium influx through these DHP-sensitive channels does not seem necessary for inducing calcium release from the sarcoplasmic reticulum (SR) (Armstrong, Bezanilla & Horowicz, 1972). Rather, it has been suggested that DHPRs operate as voltage sensors and in some way cause depolarization-induced calcium release (DICR) from the SR (Schneider & Chandler, 1973; Melzer *et al.* 1986; Rios & Brum, 1987). If only a minor portion of the DHPRs actually represent functional calcium channels (whereas the majority of receptors function as voltage sensors for DICR) a large fraction of DHPRs would not conduct Ca^{2+} ions during depolarizations (silent channels). We reinvestigated calcium currents of skeletal muscle and present evidence for excessive DHP-sensitive tail currents flowing upon repolarization from prolonged and strong depolarizations. However, we did not detect an inward or outward Ca^{2+} current during the depolarization that could account for the kinetics and voltage dependence of the excessive tails following repolarization. We interprete this in a scheme where a large subset of DHPRs remain silent during depolarizations but conduct Ca^{2+} ions during repolarization, generating large tail currents.

METHODS

Rat skeletal myoballs were prepared from newborn rats (2–5 days old) essentially as described by Beam *et al.* (1986). Briefly, for each preparation one donor animal was anaesthetized with ether and decapitated. Fore- and hind-limb muscles were minced finely and incubated in MEM medium (Gibco) containing 0·25% trypsin for 35 min at 37 °C. After washing, filtering and centrifugation the cells were resuspended in DMEM medium (Gibco) and cultured on glass coverslips where myoblasts were allowed to form myotubes. Rounded myoballs were obtained by subsequent treatment with 25 nM colchicine for 17–24 h. Patch-clamp experiments were performed in the tight-seal whole-cell configuration at 23–27 °C in an external solution containing (mM): *N*-methyl-D-glucamine, 140; KCl, 2·8; $CaCl_2$, 4; $MgCl_2$, 2; glucose, 11; TEA-Cl, 10; Hepes, 10; TTX, 0·005; pH 7·2 (equilibrated with HCl). In some experiments $CaCl_2$ was raised to 10 mM and *N*-methyl-D-glucamine replaced by NaCl. None of these substitutions altered the results reported. Patch pipettes coated with Sylgard (Dow Corning) had resistances of 1·5–3 MΩ after filling with the standard intracellular solution which contained (mM): *N*-methyl-D-glucamine, 145; NaCl, 8; $MgCl_2$, 1; Cs-EGTA, 20; Mg-ATP, 4; GTP, 0·3; Hepes 10; pH 7·2 (equilibrated with HCl). Extracellular solution changes were made by application from wide-tipped micropipettes that contained standard external solution supplemented with appropriate concentrations of PN200-110 (Sandoz, Basel, Switzerland).

Membrane currents were acquired by a computer-based patch-clamp amplifier system (EPC-9; HEKA, Lambrecht, Germany). Capacitive currents were determined and compensated before each voltage pulse using the automatic capacitance neutralization of the EPC-9. Holding potential was usually −70 mV. Currents evoked during the depolarizing test pulses are referred to as 'pulse currents'. Currents evoked upon repolarization to more negative voltages than the test pulse are referred to as 'tail currents'. Pulse and tail current amplitudes are given as peak amplitudes or in some cases as amplitudes at a specified time. Series resistance compensation was not performed. Maximal voltage errors due to membrane capacitance (C_m) and series resistance (R_s) were estimated to be about 20 mV at −70 mV with an effective limiting bandwidth of about 5 kHz and clamp times of around 273 μs (based on mean R_s values of 3·5 ± 0·3 MΩ, mean C_m values of 78 ± 11 pF ($n = 57$) and mean peak tail currents of 6·6 ± 0·9 nA ($n = 27$)). However, effects of capacitance and series resistance do not compromise the basic conclusions made here, since these would rather underestimate tail current amplitudes. Kinetic analysis was restricted to cells in which voltage errors and clamp times were less than 10 mV and faster than 200 μs. Currents were low-pass filtered at 8·8 kHz and digitized at 100 μs intervals. For analysis and presentation, currents were filtered digitally to 1–3 kHz.

The current–voltage relationships of Ca^{2+} currents were fitted with a Boltzmann function, a linear term, and a term for positive block according to:

$$I_{Ca} = g_{max}(V_m - E_{Ca}) \times \frac{1}{1 + \exp(-[V_m - V_{½}]/\text{slope})} \times \frac{1}{1 + \exp(-[V_m - V_{½\,block}]/\text{slope}_{block})},$$

where g_{max} is the maximal conductance; V_m, the test potential; E_{Ca}, the reversal potential; and $V_{½}$, the voltage at half-maximal activation. The activation curves of tail currents at 600 ms pulse duration were fitted with a single Boltzmann function according to:

$$I_{tail} = I_{max} \times \frac{1}{1 + \exp(-[V_m - V_{½}]/\text{slope})}.$$

Activation curves of tail currents measured with shorter test-pulse lengths were not fitted, as the second tail current component had not reached steady-state levels within these time limits. Activation and deactivation kinetics were approximated by biexponential fits. Throughout, data are given as means ± S.E.M. with n determinations and, where appropriate, statistical analysis was performed by applying Student's t test.

RESULTS

Ca^{2+} currents in rat skeletal myoballs

We recorded Ca^{2+} currents in rat skeletal myoballs in response to depolarizing voltage pulses with different test-pulse lengths (50, 150 and 600 ms) from a holding potential of −70 mV (Fig. 1*A*). Ca^{2+} currents were recorded in 4 mM Ca_o^{2+}, with Na^+ channels blocked by 5 μM TTX and K^+ currents inhibited by extracellular TEA (10 mM), using *N*-methyl-D-glucamine (145 mM) to replace K^+ as the intracellular monovalent cation. Voltage- and/or Ca^{2+}-activated Cl^- conductances did not interfere with Ca^{2+} currents under our experimental conditions, since the phenomena described here were found to be essentially identical when the intracellular solution contained mainly caesium glutamate (with 10 mM Cl^-) or when Ba^{2+} replaced Ca^{2+} as the charge carrier. We found Ca^{2+} currents in skeletal myoballs remarkably stable with very little rundown over tens of minutes (12 ± 6% after 20 min whole-cell recording; $n = 5$). Upon repolarizing to the holding potential, Ca^{2+} tail currents were recorded. These tail currents are thought to arise from the influx of Ca^{2+} during deactivation of Ca^{2+} channels as a consequence of the sudden increase in driving force, and their relative size should reflect the degree of channel activation during the preceding pulse. However, although the Ca^{2+} currents flowing during the test pulse (pulse currents) were maximally activated within 100 ms, the amplitude of the repolarization-induced tail currents only reached its maximal value after test-pulse durations of 600 ms. This finding conflicts with the prediction of 'normal' tail current behaviour.

Figure 1*B* plots the mean current–voltage relationship of pulse currents (measured during the last 10% of each test pulse; $n = 3$) and the peak amplitude of tail currents for a test-pulse length of 50 ms. The plot reveals the typical behaviour of high-voltage-activated Ca^{2+} channels with inward currents activating at about −30 mV, peaking around +10 mV and reversing at about +50 mV. The tail currents activate in parallel with the pulse currents but there seems to be a further increase at very depolarized

potentials. This is even more striking in Fig. 1*C*, which illustrates pulse and tail current amplitudes for depolarization lengths of 600 ms. It is obvious that the current amplitudes of the tail currents were considerably increased with longer test-pulse durations, particularly for depolarizations beyond +10 mV. It is also seen that the apparent midpoint of tail current activation shifted to the left ($V_{½} = +34 \pm 1{\cdot}7$ mV; $n = 10$; Fig. 1*C*). But even for 600 ms depolarizations it was still almost 40 mV more positive than the activation midpoint of the *I–V* curve ($V_{½} = -1 \pm 2$ mV; $n = 10$; Fig. 1*C*). Thus, during long depolarizations an additional Ca^{2+} conductance becomes evident during the deactivating phase of the Ca^{2+} channels; however, it has no kinetic counterpart during the depolarizing test pulse. This additional Ca^{2+} conductance seems to be voltage and time dependent and we will subsequently refer to this current as 'anomalous' tail current.

Kinetics of pulse and tail currents

To investigate further the time dependence of the large anomalous tails, we applied test pulses to fixed potentials but with exponentially increasing pulse durations. Figure 2 illustrates superimposed current records, evoked by test pulses to four different test-pulse potentials (0, +20, +40 and +80 mV) with varying test-pulse durations. The records reveal the progressive recruitment of anomalous tails as a function of both test-pulse potential and test-pulse duration. Figure 3*A* illustrates the mean amplitude of pulse currents of three cells, while the mean peak amplitudes of the respective tail currents measured during the deactivation phase are shown in Fig. 3*B*. If the tail currents reflected the same population of Ca^{2+} channels that were activated during the test pulse, then the tail currents would be expected to reflect faithfully the kinetics of the pulse current. This is clearly not the case for test-

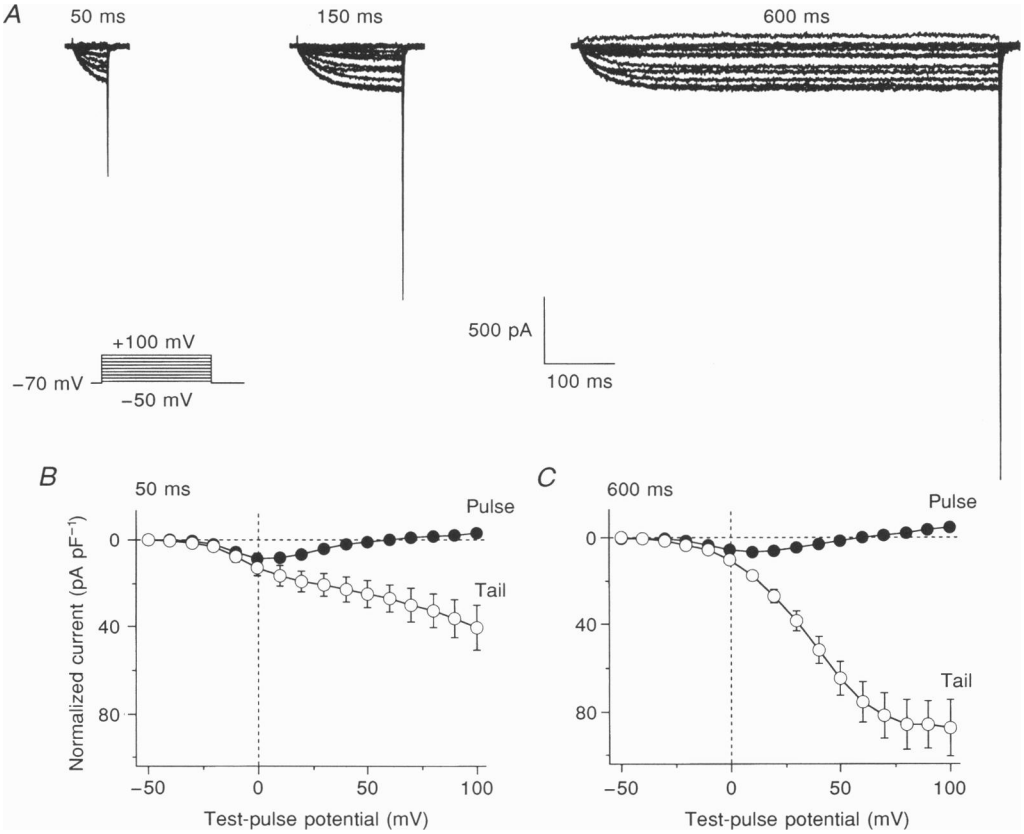

Figure 1. Continued activation of tail Ca^{2+} currents with long depolarizations

A, Ca^{2+} currents in rat skeletal myoballs evoked by depolarization to variable test-pulse potentials for 50, 150 or 600 ms from a holding potential of −70 mV. *B* and *C*, mean current–voltage relationship (●) and mean activation curve of the respective tail currents (○) obtained by a test-pulse protocol of 50 ms (*B*; $n = 3$) and 600 ms (*C*; $n = 10$). Data points of the *I–V* curve represent mean pulse current amplitudes (I_{Ca}) measured during the last 10% at the end of each test pulse as a function of test potential. The fit to the mean *I–V* curve gave the following values: $V_{½}$ (50 ms) = −7 ± 2 mV, slope (50 ms) = 5·6 ± 0·7 mV, $V_{½}$ (600 ms) = −1 ± 2 mV, slope (600 ms) = 9 ± 0·8 mV. The slope factors are statistically significant with $P < 0{\cdot}05$ (Student's *t* test). Data points of the tail current activation curve are mean peak current amplitudes (I_{tail}).

pulse potentials equal to or above +20 mV (Figs 2, 3*A* and 3*B*), as the tail current amplitudes continued to rise long after the pulse currents had peaked.

For a direct comparison, Fig. 3*C* superimposes an averaged calcium current record elicited by a test pulse to +40 mV ($n = 5$) with the time course of the respective tail current amplitudes, both normalized to peak and plotted *versus* time. At this potential, there is still inward current during the depolarization and anomalous tails are already pronounced, and it is obvious that pulse and tail currents display very different time courses. Close inspection of the activation kinetics of tail currents at +40 mV revealed a biexponential time course with time constants τ_1 and τ_2. The first time constant, τ_1, approximated 42 ± 5 ms ($n = 5$), which is in agreement with the time constant for the respective pulse current at +40 mV, ($\tau_p = 42 \pm 9$ ms). Still, the major time course of the tail current was characterized by an activation time constant that was about 7-fold slower ($\tau_2 = 270 \pm 22$ ms). Occasionally, a very fast activation process peaking within 10 ms could be resolved in the pulse currents but not the tail currents. This current was usually quite small and not further investigated as it presumably corresponds to a fast Ca^{2+} current, which has been described earlier (Beam *et al.* 1986; Cognard *et al.* 1986).

The voltage dependence of the activation time constants of pulse and tail currents is illustrated in Fig. 3*D*. The semi-logarithmic graph plots the time constant of the pulse current (τ_p) and the two time constants of the tail current (τ_1 and τ_2) *versus* their respective test-pulse potentials. The graph shows that the values for τ_p and τ_1 have similar values around 40 ms with little voltage dependence, which agrees with previously reported data in skeletal myoballs (Beam *et al.* 1986; Cognard *et al.* 1986; Cognard, Romey, Galizzi, Fosset & Lazdunski, 1986; Beam & Knudson, 1988) and presumably reflect the activation time course of so-called 'slow' Ca^{2+} channels and their corresponding tail currents. In contrast, τ_2 activates more than 10-fold slower, but accelerates at positive potentials. Activation time constants of the tail currents were quite large at moderate depolarizations ($\tau_2 = 580 \pm 160$ ms at +10 mV; $n = 5$), while at +80 mV they activated about four times faster ($\tau_2 = 147 \pm 29$ ms; $n = 5$). Even the latter time constant is considerably slower than the time constant measured for pulse currents. The kinetic discrepancy between the pulse and a large fraction of the tail currents provides strong evidence for a Ca^{2+} conductance with anomalous gating in skeletal myoballs.

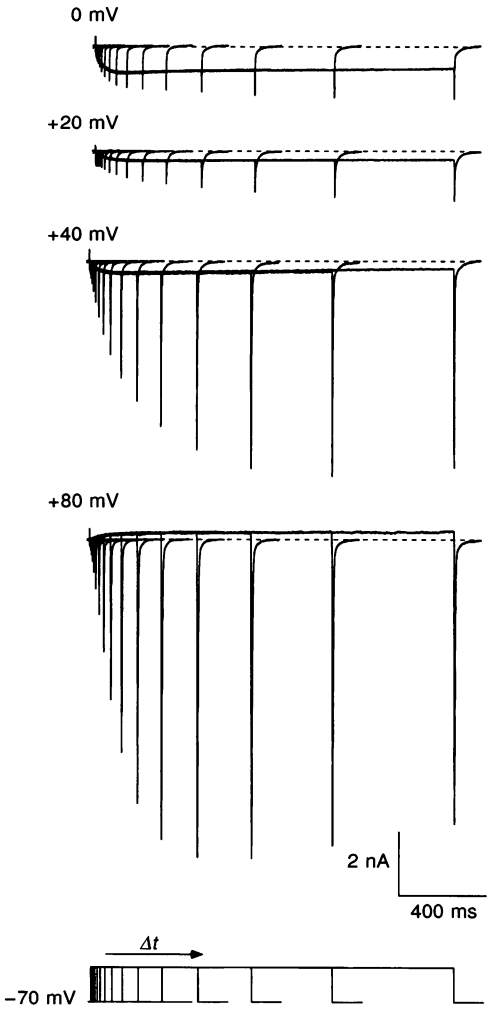

Figure 2. Time and voltage dependence of pulse and tail currents

Superimposed current records obtained by depolarizing voltage pulses to a fixed potential (0, +20, +40 or +80 mV) but exponentially increasing test-pulse lengths (all traces are from the same cell, except for those obtained at +20 mV, which were taken from a cell with similar current amplitudes).

Pulse currents show some degree of inactivation, particularly at voltages in which Ca^{2+} influx is large (e.g. at 0 mV). A quantitative assessment of pulse-current inactivation is illustrated in Fig. 3*E*, in which the inactivation time constants are plotted as a function of voltage. It is seen that inactivation is most prominent at potentials around the peak of the *I–V* curve, whereas at higher potentials (where less Ca^{2+} influx occurs), inactivation time constants increase. At potentials below 0 mV and above +40 mV, we did not observe any inactivation within the range of pulse durations applied (see e.g. Figs 1*A* and 3*A*). These data suggest that most of the inactivation is probably mediated by $[Ca^{2+}]_i$. It should be noted, however, that in experiments in which Ba^{2+} was used as charge carrier, we observed a similar if not stronger inactivation of pulse currents. This inactivation was also apparent at very positive potentials and we suspect that intracellular Ba^{2+} accumulation may have complicated side-effects on Ca^{2+} channels, which currently prevent a definitive assessment of Ca^{2+}- *versus* voltage-dependent inactivation under our experimental conditions.

Time and voltage dependence of tail current decay

Figure 4 illustrates typical tail currents at high time resolution evoked by repolarization to the indicated potentials after depolarizing pulses to +80 mV of 50 ms

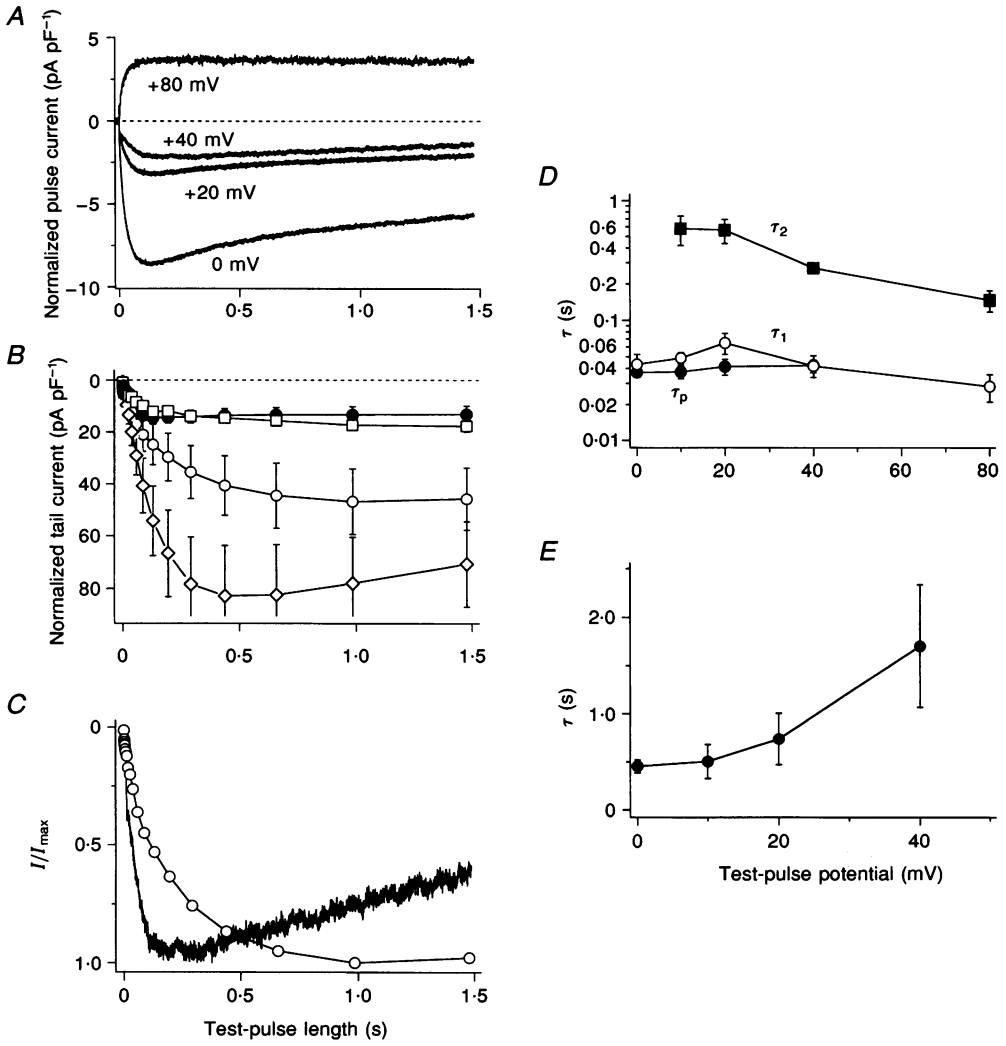

Figure 3. Time- and voltage-dependent activation of pulse and tail currents

A, mean I_{Ca} of 3 cells. Examples of 4 different test-pulse potentials are given. *B*, mean I_{tail}, measured as peak current and plotted *versus* test-pulse length ($n = 5$ each). Examples of 4 different test-pulse potentials are given (0 mV (●), +20 mV (□), +40 mV (○) and +80 mV (◇)). *C*, the mean time course of the Ca^{2+} current and the respective tail currents ($n = 5$), measured at +40 mV. Data were normalized as I/I_{max} and plotted *versus* time. *D*, semilogarithmic plot of activation time constants as a function of voltage for the pulse current τ_p (●) and the tail current τ_1 (○) and τ_2 (■). Data represent means of 5 cells. τ_p and τ_1 show no statistical differences, whereas both τ_p and τ_1 are significantly different when compared with τ_2, with $P < 0{\cdot}03$. *E*, the mean time course of pulse-current inactivation plotted as a function of test-pulse potential ($n = 3$).

(Fig. 4*A*) and 600 ms duration (Fig. 4*B*). For short depolarizations of 50 ms, we would expect that at least 70% of the classical L-type channels are activated and contribute to the tails. (Although based on the activation time constant of ~150 ms for anomalous tails at +80 mV, there might be some overlap (~30%) even for short depolarizations.) Nevertheless, when comparing the tail current amplitudes of short and long test pulses (Fig. 4*C*), it is seen that repolarization to more negative potentials yields progressively larger tail currents following the longer depolarizations. Thus, at negative repolarizing potentials, the tail current amplitudes following 600 ms depolarizations are about 3-fold larger than the corresponding tail currents induced after 50 ms, which supposedly should have already activated the majority of L-type channels (as witnessed by the activation time course of pulse currents). For comparison, the corresponding current–voltage relationship of pulse currents is superimposed with the instantaneous current–voltage relationship of the tail currents. The fit to the pulse-current *I–V* yielded a linear slope conductance of 6·6 nS, while the slope conductance of tail currents (following 600 ms depolarizations) fitted over the linear portion of the conductance was found to be about three times steeper (20 nS). This suggests that the total tail conductance is three times larger than the theoretical conductance

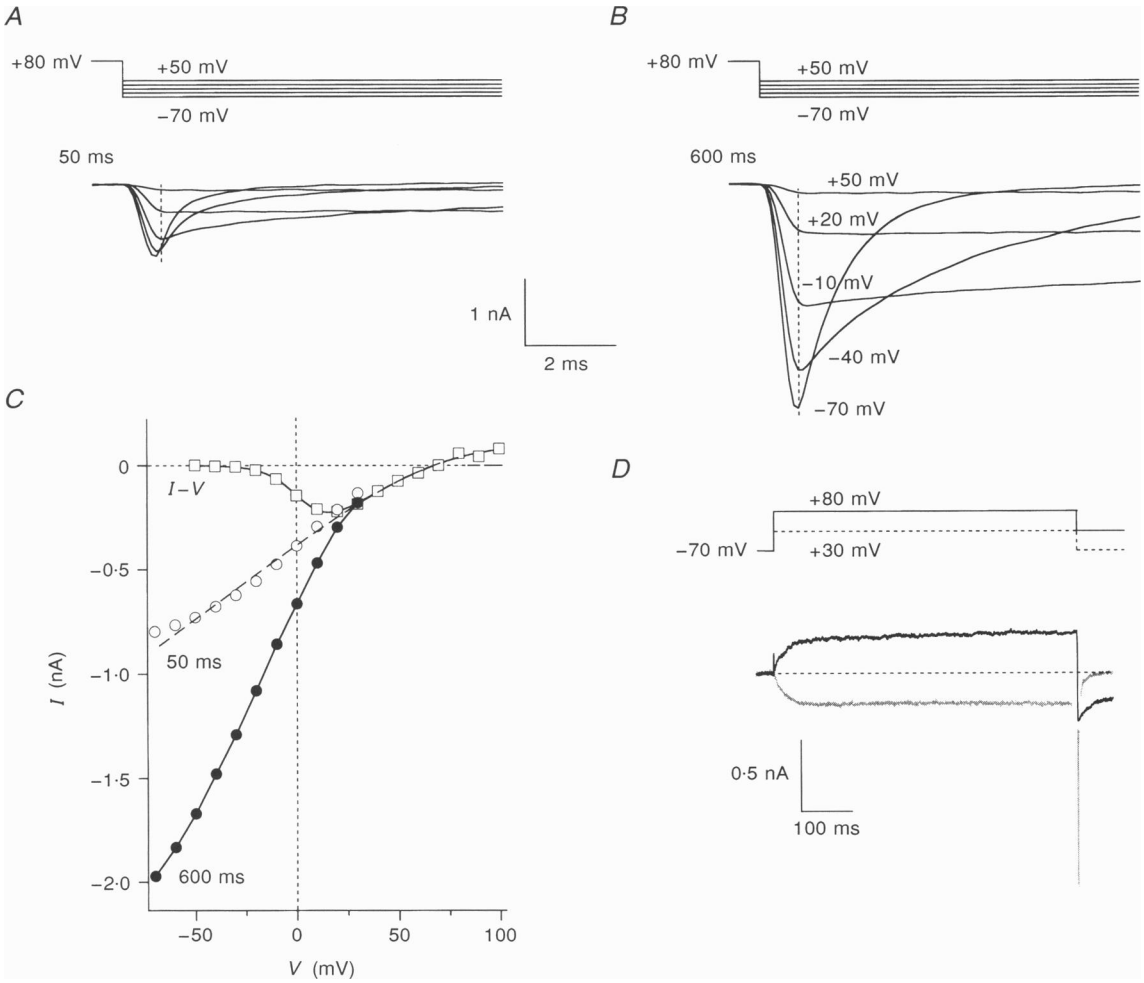

Figure 4. Instantaneous current–voltage relationships

A, tail currents evoked by depolarizations of 50 ms duration to +80 mV and repolarization to variable potentials in the range −70 to +50 mV. Holding potential was −70 mV. *B*, tail currents evoked by 600 ms depolarizations to +80 mV and repolarization to variable potentials in the range −70 to +50 mV. *C*, superimposed current–voltage relationship as a function of test-pulse potential obtained by test pulses of 600 ms duration (□) as well as mean tail current amplitudes as a function of repolarization potential following depolarizations to +80 mV for 50 ms (○) or 600 ms (●). The dashed line indicates the linear extrapolation of the slope conductance of the *I–V* relationship (as derived from g_{max} of an *I–V* fit). Data points were measured at the same point in time after repolarization (as indicated by the dashed vertical line in *A* and *B*). Data are from the same 3 cells. *D*, superimposed raw data traces evoked by depolarizations of 600 ms to +30 mV and repolarization to −70 mV (grey trace) and to +80 mV followed by repolarization to +30 mV. Traces are from the same cell.

expected from the pulse currents, bearing in mind that we are likely to have underestimated the amplitude of tail currents due to clamp-speed limitations. This relationship might give a rough estimate of the ratio of anomalous *versus* 'normal' Ca^{2+} channels (see Discussion).

Could the anomalous tail current component be attributable to a modal gating behaviour of Ca^{2+} channels? Such modal gating has been observed in cardiac cells, where strong and prolonged depolarizations altered the open probability of L-type Ca^{2+} channels (Pietrobon & Hess, 1990). Although this type of modal gating has not yet been demonstrated for skeletal muscle Ca^{2+} channels, if it were present, it might explain anomalous tail current behaviour in the context of an increased open probability of 'normal' Ca^{2+} channels. Figure 4*D* superimposes and compares the amplitude of the Ca^{2+} current evoked by a simple depolarizing voltage pulse to +30 mV and the amplitude of the Ca^{2+} current at this potential following a long-lasting prepulse to +80 mV for 600 ms. If the prepulse had altered the open probability of Ca^{2+} channels one would expect a larger current amplitude following the prepulse. However, the fact that the prepulse did not significantly increase the amplitude of the inward current recorded at +30 mV suggests that the open probability of skeletal muscle Ca^{2+} channels is not modified by strong and long-lasting depolarizations and that modal gating is not likely to be manifest under our experimental conditions.

As evident from the current records in Fig. 4*A* and *B*, the time course of decay of tail currents was slow at positive potentials but became progressively faster at more negative repolarizing potentials. We have not attempted a detailed quantitative analysis of the decay kinetics of tail currents in this study, since many cells showed complex and variable deactivation kinetics, presumably due to the combined effects of imperfect voltage control, the large amplitudes of tail currents, and Ca^{2+}-dependent inactivation. However, we have succeeded in obtaining data from a few cells with small capacitance and low series resistance (mean capacitance, $22{\cdot}8 \pm 2{\cdot}1$ pF; mean R_s, $3{\cdot}6 \pm 0{\cdot}4$ MΩ; $n = 5$) yielding clamp speeds around 80 μs and maximal voltage errors below 12 mV (mean peak tail current, 3·3 nA). Figure 5 illustrates the decay of tail currents in such small cells. In Fig. 5*A* and *B*, the tail currents were obtained by repolarizations to −70 mV, activated by short (50 ms) or long (600 ms) depolarizations to +80 mV. At such negative repolarization potentials, the decay phase was very rapid for both depolarization protocols. The time constants were largely accounted for by a single exponential with time constants of $1{\cdot}3 \pm 0{\cdot}3$ ms for short depolarizations and 3 ± 2 ms for long depolarizations. There was a minor slow component, whose amplitude was on average less than 10% of the total tail current amplitude.

It has been suggested that a slowing of deactivation might account for an apparent increase in tail currents (Nakayama & Brading, 1993*a*). Although our experiments indeed revealed a slowing of deactivation with prolonged depolarizations, this effect is certainly too small to account for a 3-fold increase in tail current amplitude. As stated above, the experimental conditions provided clamp speeds of 80 μs and we measured a tail current deactivation time constant of 1·3 ms following short depolarizations. Based on these premises, a theoretical bi-exponential fit would predict the size of the measured peak tail current to resolve about 80% of the true peak tail current amplitude. Assuming the same maximal tail current amplitude, a slower deactivation of 3 ms (as measured following longer depolarizations) would indeed allow a better resolution of the measured tail currents and yield about 90% of the true peak current. However, this difference is not substantial and would only produce an apparent increase in tail current amplitude of less than 15%. Furthermore, this apparent increase is more likely to be counteracted by the voltage error of about 10 mV which inevitably occurs when tail currents become very large, as is the case for long depolarizations. In fact, we assume that this effect will attenuate tail currents following long depolarizations more than will the faster deactivation following short depolarizations.

In order to minimize the inaccuracies involved in fast tail current kinetics, we took advantage of the fact that deactivation kinetics of tail currents are very much slowed by less negative repolarizations (see Fig. 4*A* and *B*). Figure 5*C* illustrates typical examples of tail currents evoked by repolarizations to −30 mV following 600 ms prepulses to various potentials. It is seen that the decay of these tail currents exhibited primarily a slow time course, which allows for a rather accurate assessment of the tail current amplitudes. In three cells, the predominant slow component had a time constant of 20–30 ms. At moderate depolarizations, there was also a discernible albeit small 'fast' component that had a mean time constant of 3–7 ms. With stronger depolarizations, however, this component submerged in the large amplitude increase of the slow component. The mean tail current amplitudes of five cells measured at repolarizing potentials of −30 mV as a function of the depolarizing prepulse of 600 ms are shown in Fig. 5*D*. For comparison, a plot of the tail current amplitudes for shorter depolarizations of 50 ms is also shown ($n = 3$).

Thus, even under conditions of slow deactivation, there was a time-dependent increase in the tail currents when subjecting the cells to depolarizing voltage pulses of +80 mV for increasing durations and subsequent repolarization to −30 mV. As seen in the example of Fig. 5*E*, the deactivation behaviour of the tail currents was similar to that described above (cf. Fig. 5*C*). There was a large increase in the tail current amplitude with longer depolarizations due to the augmentation of a slowly deactivating tail current component. The mean time course

of the peak tail current amplitude of five cells is plotted in Fig. 5*F*, which reveals a bi-exponential time course with a fast time constant of 58 ± 9 ms and a slow time constant of 396 ± 101 ms.

Together, these data exclude the lack of adequate temporal resolution or a simple kinetic slowing of the tails as the cause of the excessive tail currents. Instead, they substantiate the notion that strong and long depolarizations promote the recruitment of a subset of Ca^{2+} channels with anomalous gating rather than modal gating or a second open state. The data obtained at mild repolarizations also tend to suggest that the slow component is likely to be due to tail currents associated with the anomalously gated Ca^{2+} channels, whereas the fast deactivating tail currents might correspond to the classical L-type Ca^{2+} channels. At more negative repolarizations, both components deactivate at maximal rates and the differences are less pronounced.

Steady-state inactivation

In a further series of experiments, we investigated the steady-state inactivation properties of pulse and tail currents. The experimental protocol used to assess the inactivation of pulse currents was as follows. A long

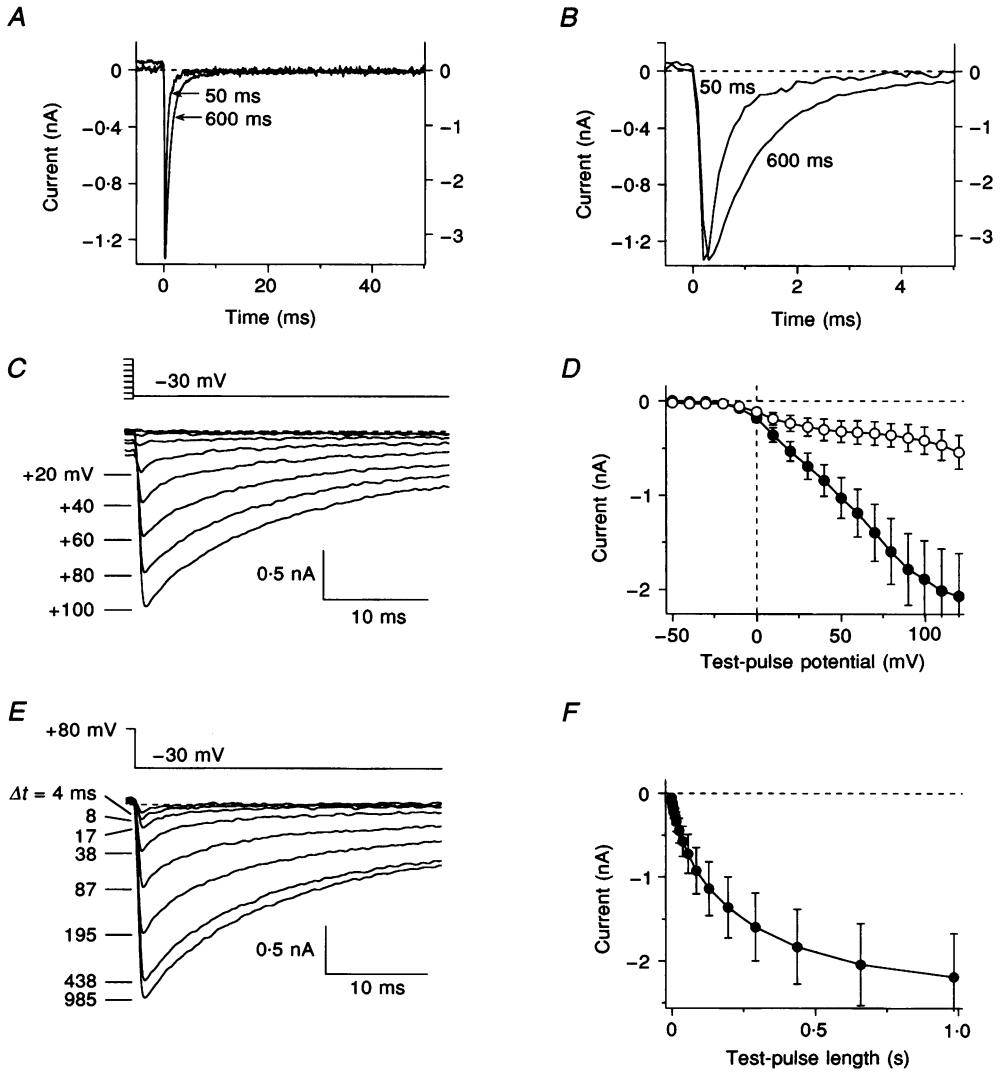

Figure 5. Deactivation characteristics of tail currents

A, superimposed tail currents from the same cell evoked by repolarization to −70 mV following depolarizations to +80 mV for 50 ms (left ordinate) and 600 ms (right ordinate). *B*, same as *A* on an expanded time scale. *C*, superimposed tail currents evoked repolarization to −30 mV following 600 ms test pulses to variable potentials. *D*, mean activation curves of tail currents recorded at repolarization potentials of −30 mV following depolarizing pulses to +80 mV for durations of 50 ms (○; $n = 3$) or 600 ms (●; $n = 5$). Data points were measured as described in Fig. 1*B*. *E*, superimposed tail currents evoked by repolarization to −30 mV following depolarizations to +80 mV with exponentially increasing durations. Same cell as in *C*. *F*, mean I_{tail}, measured as peak current and plotted *versus* test-pulse length ($n = 5$). Repolarization potential was −30 mV.

conditioning pulse of 5 s duration to variable potentials was followed by a 50 ms test pulse to +10 mV. The long conditioning pulse was designed to accomplish steady-state inactivation and the subsequent pulse to +10 mV was aimed at testing the degree of pulse-current inactivation. Superimposed records of three pulse currents evoked by the test pulse following conditioning pulses to −80, −20 and +80 mV are illustrated in Fig. 6*A* and the mean pulse-current amplitudes of three cells subjected to a wide range of conditioning pulses is depicted in Fig. 6*C*. The resulting steady-state inactivation curve was U-shaped. The U-shaped inactivation curve of pulse currents supports our previous conclusion that most of the inactivation (albeit incomplete) is likely to be due to Ca^{2+}-induced inactivation. At very positive conditioning pulses, pulse-current amplitudes were slightly larger than at hyperpolarized potentials. This is presumably due to incomplete activation of pulse currents during the 50 ms test pulse to +10 mV from potentials more negative than this test voltage. We have therefore normalized the pulse currents to the amplitude obtained at +10 mV after a conditioning pulse to +80 mV, at which potential there is almost complete activation of pulse currents. We cannot entirely rule out a small voltage-dependent inactivation, since we observed a small reduction of pulse currents already at potentials that normally failed to generate large Ca^{2+} influx (e.g. at −50 mV).

To assess the steady-state inactivation behaviour of tail currents, we modified the above protocol such that following the conditioning pulse, there was a 50 ms pulse to +80 mV, which was aimed at producing an almost full activation of pulse currents (at least 70% activation based

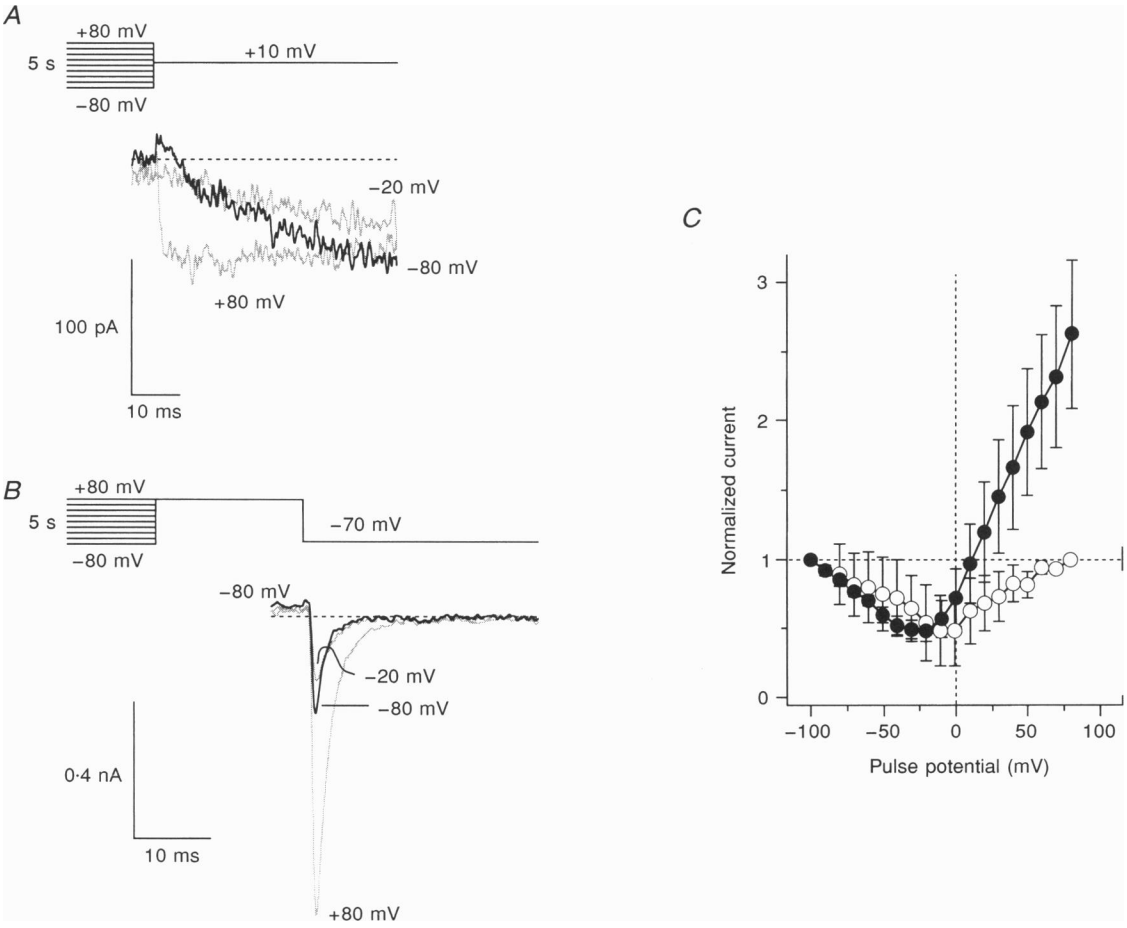

Figure 6. Steady-state inactivation of I_{Ca} and I_{tail}

A, superimposed current records evoked by repolarization to +10 mV following variable conditioning prepulses of 5 s duration to the indicated potentials. *B*, superimposed data traces evoked by repolarization to −70 mV following a test pulse to +80 mV and 50 ms durations, which was preceded by variable conditioning prepulses of 5 s duration to the indicated potentials. Same cell as in *A*. *C*, superimposed steady-state inactivation curve of pulse (○; $n = 3$) and tail currents (●; $n = 5$) plotted as a function of conditioning potential. Mean pulse–current amplitudes were measured at +10 mV during the last 10% of the 50 ms test pulse and normalized to the current obtained at +80 mV. Mean tail currents were measured as peak amplitudes at −70 mV and normalized to the tail current measured at −100 mV.

on the activation kinetics of the fast tail current component), but without causing too strong an activation of the slower anomalous tails. The resulting tail currents were measured at −70 mV and examples of such tail currents are depicted in Fig. 6*B* for various conditioning pulses (−80, −20 and +80 mV). Similar to the pulse currents, tail current amplitudes were decreased following conditioning depolarizations below −30 mV. Depolarizations beyond this potential did not further reduce the tail currents, but progressively increased tail current amplitudes up to at least 3-fold above the control level. The fact that tail currents can increase several-fold beyond the control levels further strengthens the argument that strong depolarizations recruit anomalous Ca^{2+} channels which give rise to excessive tail currents. It is notable that the bell-shaped curve of the tail currents has its minimum shifted to more negative values than the pulse-current curve. This is presumably due to the activation of anomalous tail currents at potentials around −10 mV, which start to overcome the Ca^{2+}-induced inactivation of the 'normal' tail currents associated with the classical L-type channels activated during the pulse.

Blocking effects of dihydropyridines

Neuronal and skeletal muscle L-type Ca^{2+} channels are potently blocked by dihydropyridines (DHPs) (Cognard *et al.* 1986; Porzig, 1990). In myoballs, the Ca^{2+} channel antagonist PN200-110 completely blocked both pulse and tail currents at 1 μM concentration ($n = 3$, data not shown), suggesting that both slow Ca^{2+} currents as well as anomalous tail currents are sensitive to DHPs. Suppression of Ca^{2+} currents by DHPs is known to be voltage dependent and expected to be more effective at positive potentials (Bean, 1984). Application of lower concentrations of PN200-110 revealed this well-known voltage dependence of DHP block. Figure 7*A* and *B* plots the mean current–voltage relationship of pulse currents and the corresponding tail currents ($n = 3$) before and 5 min after application of 100 nM PN200-110 (5 min being the time required to achieve steady-state block). This concentration of PN200-110 reduced both peak pulse currents and tail currents by 20–60% in a voltage-dependent manner. Figure 7*C* illustrates the similarity in the degree of block obtained at the various potentials for both pulse and tail currents. This provides evidence that the slow Ca^{2+} currents

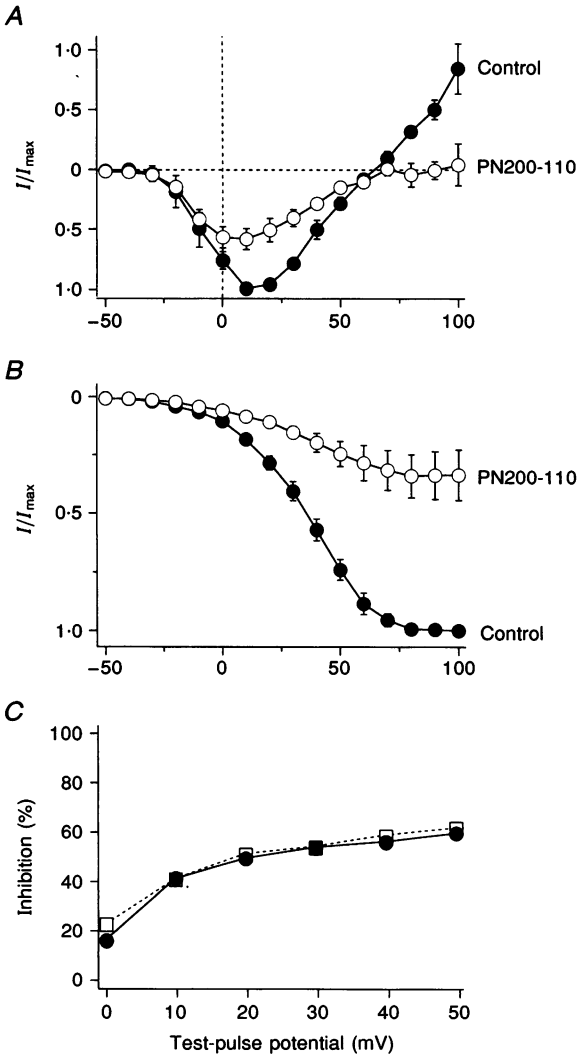

Figure 7. Effects of dihydropyridines on I_{Ca} and I_{tail}
A, mean current–voltage relationship obtained by depolarizations to variable test-pulse potentials of 150 ms from a holding potential of −70 mV ($n = 3$). Data plotted are before (●) and after 5 min of 100 nM PN200-110 exposure (○). Data were normalized as I/I_{max}. *B*, mean I_{tail} (taken as I/I_{max}) from the same cells as in *A*, evoked by repolarization to −70 mV and plotted as a function of test-pulse potential. The data show I_{tail} before (●) and after 100 nM PN200-110 application (○). Data were normalized as I/I_{max}. *C*, percentage inhibition of pulse (●) and tail (□) currents after 5 min of PN200-110 exposure, plotted as a function of test-pulse potential.

as well as the additional Ca^{2+} conductance of tail currents are carried by DHP-sensitive Ca^{2+} channels.

DISCUSSION

The present study of Ca^{2+} currents in skeletal muscle clearly establishes divergence in the behaviour of pulse currents activated by depolarization and tail currents following repolarization. The differences concern both voltage dependence and kinetics and may be summarized as follows. (1) Pulse currents show the classical voltage dependence of high-voltage-gated L-type Ca^{2+} channels, whereas tail currents are activated in a biphasic manner with a small component that matches the activation of pulse currents and an additional component that is activated at significantly more positive potentials. (2) Pulse current kinetics show a single activation time constant of ~40 ms, whereas tail currents show two components (~50 ms and 150–600 ms). The major question in view of the present results is whether the discrepancies between pulse and tail currents are attributable to a single population of Ca^{2+} channels or to two distinct types of channels with different properties and possibly different functions. Although we favour the latter interpretation, it seems appropriate to first discuss possible scenarios that would explain the anomalous behaviour of tail currents based on known properties of L-type Ca^{2+} channels.

If one assumed a single population of Ca^{2+} channels, one would have to postulate that the deviation in the activation kinetics of pulse and tail currents is only an apparent one. One would have to argue that the determination of the true activation time course of pulse currents is compromised by the simultaneously occurring inactivation, which curtails the ongoing activation and yields apparently fast activation kinetics. This is highly unlikely, since under our experimental conditions (20 mM intracellular EGTA) inactivation of pulse currents is rather small and slow (time constants $>$ 500 ms). Furthermore, there seems to be little if any inactivation at potentials more positive than +40 mV (see e.g. Figs 1 and 3), which is the voltage at which the anomalous tail currents become very prominent. Outward currents at these positive potentials are almost certainly through Ca^{2+} channels (presumably carried by Cs^{+} ions), since they are blocked by DHPs (see Fig. 7), and it is likely that the observed fast time course of these outward currents truly reflects rapid and mono-exponential activation kinetics. Additional evidence for rather fast activation of pulse currents comes from the fact that tail currents clearly exhibit two activation components, one of which closely matches the activation time course of the pulse currents. Together, this argues against an apparent speeding of the activation of pulse currents by inactivation and suggests that tail currents accurately reflect the activation of tails corresponding to the pulse currents with an additional component that is significantly slower, but does not have a kinetic counterpart in the pulse currents. This might be considered as 'anomalous' gating of Ca^{2+} channels since it requires depolarization in the absence of detectable current flow (either inward Ca^{2+} or outward Cs^{+} current) during depolarization, but the current through these channels becomes apparent only as the membrane is repolarized.

Anomalous gating of Ca^{2+} channels has been observed in several studies. A low open probability of Ca^{2+} channels during depolarization followed by an increased open probability during repolarization has been reported in cerebellar granule and hippocampal neurons (Fisher, Gray & Johnston, 1990; Slesinger & Lansman, 1991; Forti & Pietrobon, 1993), where the phenomenon has been interpreted as resulting from an altered gating mode of classical DHP-sensitive L-type Ca^{2+} channels (Forti & Pietrobon, 1993) or by transitions of deactivated channels through an open state before returning to the closed state (Fisher *et al.* 1990; Slesinger & Lansman, 1991). The anomalous tail currents shown here are unlikely to correspond to the channel activity in those cells, since the tail currents described in our study conduct instantaneously (the rise time of tail currents is less than 100 μs and essentially limited by clamp speed) and have extremely short deactivation time constants (about 3 ms at −70 mV). This is in contrast to the characteristics of channels described in hippocampal and cerebellar neurons where a delay of several milliseconds in the onset of channel activity is prominent and the high probability of repolarization openings can last tens to hundreds of milliseconds (Fisher *et al.* 1990; Slesinger & Lansman, 1991; Forti & Pietrobon, 1993).

In cardiac myocytes, strong and long-lasting depolarizations drive L-type Ca^{2+} channels into a mode of gating that is characterized by long openings and high open probability (Pietrobon & Hess, 1990). In this case, the channels appear to shift into this mode during the depolarization, since immediately after repolarization, an increased open probability with long-lasting open times and a very slow return to the normal gating mode was observed. Such modal gating behaviour is apparently not manifest in skeletal muscle under our experimental conditions, since we found no increase in conductance during long depolarizations to positive potentials. If channels indeed would change their open probability, then we would expect to detect this as both an increase in outward current with kinetics that match the activation of the anomalous tails and as an increased conductance upon repolarization to positive potentials, where escape from this long-lived state would be slow (see Fig. 4*D*). Clearly, neither of these predicted characteristics of modal behaviour were found in our experiments.

Probably the closest qualitative resemblance to our present results is found in experiments in smooth muscle cells (Nakayama & Brading, 1993*a*, *b*), where tail currents also increased with stronger depolarization and/or progressive

depolarization times. The fact that tail current deactivation in smooth muscle cells became slower with increasing depolarizations or longer depolarizations, led the authors to interprete the tail current behaviour as resulting from a single population of Ca^{2+} channels with two open states. In order to make this hypothesis of a second open state applicable to our data, one would have to assume the following: (1) there is one homogeneous population of Ca^{2+} channels that enters the first open state with the voltage dependence and kinetics of the recorded pulse currents; (2) strong and/or long depolarizations will shift these Ca^{2+} channels into a second open state (without changing the overall open probability); (3) the second open state is left more slowly and causes a slower deactivation of tails; and (4) the tails of the first open state might not be resolved accurately, because of its fast deactivation, whereas the second open state produces 'anomalous' tails, because it is long enough to be temporally resolved. In other words, the anomalous tails are actually the reflection of a 'missed' first open state rather than the recruitment of an additional current component.

We do not consider this as a likely explanation for the phenomena observed in the present study, because the manifestation of anomalous tails was not restricted to very negative repolarizations (at which tail currents indeed have fast deactivation time constants). Even at less negative potentials such as −30 mV (see Fig. 5), we still observed a large increase in the amplitude of tail currents by strong depolarizations and/or prolonged depolarizations. Under these conditions, in which deactivation kinetics do not compromise an accurate assessment of tail current amplitudes, it is very clear that the already slow deactivation kinetics are not grossly altered but that it is mainly the amplitude that is increased (by at least 3-fold).

Since our data cannot easily be incorporated in the schemes of known gating behaviours of L-type Ca^{2+} channels, we would like to consider the following, admittedly speculative, interpretations for the excessive tail currents. (1) *Anomalous permeation properties*: one could assume a normal open probability during depolarizations but the absence of current might result from a tight binding and co-ordination of Ca^{2+} ions in the channel pore that would prevent permeation at positive potentials. A 'punch through' of the trapped Ca^{2+} ion during repolarization might then cause permeation through the channels. (2) *Permeation block*: here, the permeation of Ca^{2+} is not impaired by the Ca^{2+} ion *per se*, but through a 'blocking particle' of unknown nature that prevents Ca^{2+} influx during depolarization, presumably from the cytosolic side. Upon repolarization, we must assume a rapid unblock that allows tail current flow. An attractive candidate for such a 'blocking particle' is the ryanodine receptor, which is thought to interact with DHP receptors during excitation–contraction (E–C) coupling. At present we do not know if Ca^{2+} channels producing anomalous tail currents are also capable of carrying inward current under certain circumstances, in which case they might behave like 'normal' Ca^{2+} channels. In this context it is noteworthy that L-type Ca^{2+} channels in skeletal muscle are subject to facilitation by voltage- and frequency-dependent processes, apparently mediated by cAMP-dependent phosphorylation (Sculptoreanu, Scheuer & Catterall, 1993). Additional studies should clarify if this facilitation is related to the anomalous tail currents described here.

The present data suggest the presence of a DHP-sensitive type of Ca^{2+} channel with anomalous gating, which conducts Ca^{2+} only during the deactivation phase of Ca^{2+} channels in the form of large tail currents. These anomalous-gated Ca^{2+} channels might indeed represent voltage sensors in E–C coupling previously thought to be non-conducting DHPRs. It was originally proposed that there might be 35–50 times more DHP-binding sites than conducting Ca^{2+} channels (Schwartz, McCleskey & Almers, 1985), an estimate that presumably exaggerates the true relationship by assuming a channel open probability of one. A thorough discussion of the issues relating to the stochiometry of DHP-binding sites and functional Ca^{2+} channels (Lamb & Walsh, 1987) indicates that there still might be 'silent' channels albeit not as abundant as originally suggested. Presuming a homogeneous Ca^{2+} channel population, we estimated the theoretical conductance of the tail currents to be 6·6 nS (extrapolated from the g_{max} of the I–V fit and assuming linear conductance for Ca^{2+} channels at negative potentials; Fig. 4*C*). However, the measured tail current conductance after 600 ms of depolarization was 20 nS (Fig. 4*C*). This would correspond to a ratio of tail *versus* pulse current of about 3. If tail currents and pulse currents have similar single-channel conductances (and disregarding the likely underestimation of tail currents due to series resistance and membrane capacitance), then these estimates would roughly yield a proportion of at least two to three anomalous-gated Ca^{2+} channels per normal conducting L-type channel. We should stress, however, that these estimates are tentative at best as they are based on assumptions that require substantiation.

The functional role of the DHPRs underlying the anomalous tail currents is presently unknown, but might well involve activation or inactivation of E–C coupling. It remains to be established, whether anomalous Ca^{2+} channels act as voltage sensors in E–C coupling and how the excess number of channels relate to a hypothesis that suggests that each alternate calcium release channel is associated with a tetrad of DHPRs (Block, Imagawa, Campbell & Franzini-Armstrong, 1988) and to the observation that calcium release seems to be controlled by the movement of four identical charged units (Simon & Hill, 1992). On the other hand, the striking coincidence of the rather slow activation of anomalous tail currents with the time course of the recently described phenomenon of

repolarization-induced stop of calcium release (RISC) in the same preparation (Suda & Penner, 1994) might point to a role of anomalous tail currents in terminating Ca^{2+} release. Alternatively, these channels could function as reserve Ca^{2+} channels that may be recruited by high-frequency stimulation of muscle cells.

Armstrong, C. M., Bezanilla, F. M. & Horowicz, P. (1972). Twitches in the presence of ethylene glycol bis(β-amino ethyl ether)-*N,N'*-tetraacetic acid. *Biochimica et Biophysica Acta* **267**, 605–608.

Beam, K. G. & Knudson, C. M. (1988). Calcium currents in embryonic and neonatal mammalian skeletal muscle. *Journal of General Physiology* **91**, 781–798.

Beam, K. G., Knudson, C. M. & Powell, J. A. (1986). A lethal mutation in mice eliminates the slow calcium current in skeletal muscle cells. *Nature* **320**, 168–170.

Bean, B. P. (1984). Nitrendipine block of cardiac calcium channels: high affinity binding to the inactivated state. *Proceedings of the National Academy of Sciences of the USA* **81**, 6388–6392.

Block, B. A., Imagawa, T., Campbell, K. P. & Franzini-Armstrong, C. (1988). Structural evidence for direct interaction between the molecular components of the transverse tubule/sarcoplasmic reticulum junction in skeletal muscle. *Journal of Cell Biology* **107**, 2587–2600.

Cognard, C., Lazdunski, M. & Romey, G. (1986). Different types of Ca^{2+} channels in mammalian skeletal muscle cells in culture. *Proceedings of the National Academy of Sciences of the USA* **83**, 517–521.

Cognard, C., Romey, G., Galizzi, J.-P., Fosset, M. & Lazdunski, M. (1986). Dihydropyridine-sensitive Ca^{2+} channels in mammalian skeletal muscle cells in culture: electrophysiological properties and interactions with Ca^{2+} channel activator (Bay K8644) and inhibitor (PN 200-110). *Proceedings of the National Academy of Sciences of the USA* **83**, 1518–1522.

Donaldson, P. L. & Beam, K. G. (1983). Calcium currents in fast-twitch skeletal muscle of the rat. *Journal of General Physiology* **82**, 449–468.

Fisher, R. E., Gray, R. & Johnston, D. (1990). Properties and distribution of single voltage-gated calcium channels in adult hippocampal neurons. *Journal of Neurophysiology* **64**, 91–104.

Forti, L. & Pietrobon, D. (1993). Functional diversity of L-type calcium channels in rat cerebellar neurons. *Neuron* **10**, 437–450.

Lamb, G. D. (1992). DHP receptors and excitation-contraction coupling. *Journal of Muscle Research and Cell Motility* **13**, 394–405.

Lamb, G. D. & Walsh, T. (1987). Calcium currents, charge movement and dihydropyridine binding in fast- and slow-twitch muscles of rat and rabbit. *Journal of Physiology* **393**, 595–617.

Melzer, W., Schneider, M. F., Simon, B. J. & Szucs, G. (1986). Intramembrane charge movement and calcium release in frog skeletal muscle. *Journal of Physiology* **373**, 481–511.

Nakayama, S. & Brading, A. F. (1993*a*). Evidence for multiple open states of the Ca^{2+} channels in smooth muscle cells isolated from the guinea-pig detrusor. *Journal of Physiology* **471**, 87–105.

Nakayama, S. & Brading, A. F. (1993*b*). Inactivation of the voltage-dependent Ca^{2+} channel current in smooth muscle cells isolated from the guinea-pig detrusor. *Journal of Physiology* **471**, 107–127.

Pietrobon, D. & Hess, P. (1990). Novel mechanism of voltage-dependent gating in L-type calcium channels. *Nature* **346**, 651–655.

Porzig, H. (1990). Pharmacological modulation of voltage-dependent calcium channels in intact cells. *Reviews in Physiology, Biochemistry and Pharmacology* **114**, 209–262.

Rios, E. & Brum, G. (1987). Involvement of dihydropyridine receptors in excitation-contraction coupling in skeletal muscle. *Nature* **325**, 717–720.

Rios, E. & Pizarro, G. (1991). Voltage sensor of excitation-contraction coupling in skeletal muscle. *Physiological Reviews* **71**, 849–908.

Schneider, M. F. & Chandler, W. K. (1973). Voltage dependent charge movement in skeletal muscle: a possible step in excitation-contraction coupling. *Nature* **242**, 244–246.

Schwartz, L. M., McCleskey, E. W. & Almers, W. (1985). Dihydropyridine receptors in muscle are voltage-dependent but most are not functional calcium channels. *Nature* **314**, 747–751.

Sculptoreanu, A., Scheuer, T. & Catterall, W. A. (1993). Voltage-dependent potentiation of L-type Ca^{2+} channels due to phosphorylation by cAMP-dependent protein kinase. *Nature* **364**, 240–243.

Simon, B. J. & Hill, D. A. (1992). Charge movement and SR calcium release in frog skeletal muscle can be related by a Hodgkin-Huxley model with four gating particles. *Biophysical Journal* **61**, 1109–1116.

Slesinger, P. A. & Lansman, J. B. (1991). Reopening of Ca^{2+} channels in mouse cerebellar neurons at resting membrane potentials during recovery from inactivation. *Neuron* **7**, 755–762.

Suda, N. & Penner, R. (1994). Membrane repolarization stops caffeine-induced Ca^{2+} release in skeletal muscle cells. *Proceedings of the National Academy of Sciences of the USA* **91**, 5725–5729.

Acknowledgements

We thank Frauke Friedlein and Michael Pilot for technical assistance. We thank Graham D. Lamb, Erwin Neher and Anant Parekh for critical discussions and comments on the manuscript. We acknowledge support by the following institutions: Deutsche Forschungsgemeinschaft, Sonderforschungsbereich 236, Hermann- und Lilly-Schilling-Stiftung.

Received 13 February 1995; accepted 15 May 1995.